

MET.O.14

METEOROLOGICAL OFFICE
BOUNDARY LAYER RESEARCH BRANCH
TURBULENCE & DIFFUSION NOTE



T.D.N. No. 119

Preliminary Results on Neutral Integration with
with a Change in Surface Roughness.

by

C.A.Nash

April 1980

Please note: Permission to quote from this unpublished note should be
obtained from the Head of Met.O.14, Bracknell, Berks, U.K.

FH1B

1. Introduction

We consider the behaviour of the surface stress in a neutral atmospheric boundary layer flowing over a terrain that has a slowly changing roughness, in the sense that the roughness length z_0 is locally well defined but will vary substantially on the scale of the periodic domain.

This is a problem of concern to micrometeorologists and atmospheric modellers, who in particular need to know on what scales a simple extrapolation of horizontally homogeneous theory is appropriate.

Many workers have considered an infinite domain with a single step change in surface roughness, but none have looked at the periodic case. Taylor (1969) used a mixing length model, with $l = k(z + z_0)$ and Petersen (1969) used a one equation turbulence model with $-\overline{uw} = K \cdot q$ (q is the turbulence kinetic energy) to examine the step change problem. Rao et al (1974) applied a modified version of their group's second order closure model to the same problem.

All these attempts used the steady equations with the hierarchy of closures described, but neglected $\partial p / \partial x$ in the horizontal momentum equation thus producing a parabolic set of equations that could be integrated steadily downstream. However this prevents any upstream influence which may be significant particularly in the vicinity of the step change where $\partial p / \partial x$ is known to be large. Further work hopes to look at this more closely

Shir (1972) used a turbulent energy equation model in which the pressure gradients were retained. The effect on the surface stress evolution with distance was not greatly affected. However his upstream boundary condition does not allow upstream influence.

Also each worker used his model to examine the assumptions implicit in the parameterisations lower in the hierarchy. The mixing length model of Taylor implies that the non-dimensional wind shear $\phi_m = \frac{Kz}{u_*} \cdot \frac{\partial u}{\partial z}$ is identically unity throughout the height of his model; this is the equilibrium result and is in error by up to 50% in non-equilibrium flows of this type. Rao et al were also able to look at $\frac{-\overline{uw}}{q}$ and found variations of up to 30%, from its implied constant value in the one equation models. However the models agree to

a surprising extent despite their differences.

More importantly, all these models are surface layer which impose the upstream boundary conditions as $z \rightarrow \infty$ for all distances downstream of the roughness change. Thus the boundary layer cannot asymptote to the equilibrium profile that would be expected physically as $x \rightarrow \infty$. The model described here is a deep model and does not impose such an artificial upper boundary condition.

Also the pressure gradients are retained throughout and the results should be uniformly valid subject only to resolution limitations.

We will show that the surface layer models suggest the solution quantitatively in the case of periodic roughness changes on the scales we study, where the flow appears predominantly parabolic, and in particular gives the correct length scale on which the stress changes.

The model and turbulence parameterisations are described in section 2 followed in section 3 by a description of results. Some conclusions are collected in section 4.

2. Description of model integration

The model is a 2-D time dependent Navier-Stokes equation code in which the viscosity can be parameterised in various ways. The basic equations are

$$\begin{aligned} \frac{\partial u}{\partial t} + u \frac{\partial u}{\partial x} + w \frac{\partial u}{\partial z} &= -\frac{\partial p}{\partial x} + f^v + \frac{\partial}{\partial x} \left(2\nu_x \frac{\partial u}{\partial x} \right) + \frac{\partial}{\partial z} \left(\nu_x \frac{\partial u}{\partial z} + \nu_x \frac{\partial w}{\partial x} \right) \\ \frac{\partial v}{\partial t} + u \frac{\partial v}{\partial x} + w \frac{\partial v}{\partial z} &= -\frac{\partial p}{\partial y} - f^u + \frac{\partial}{\partial x} \left(\nu_x \frac{\partial v}{\partial x} \right) + \frac{\partial}{\partial z} \left(\nu_x \frac{\partial v}{\partial z} \right) \\ \frac{\partial w}{\partial t} + u \frac{\partial w}{\partial x} + w \frac{\partial w}{\partial z} &= -\frac{\partial p}{\partial z} + \frac{\partial}{\partial x} \left(\nu_x \frac{\partial w}{\partial x} + \nu_x \frac{\partial u}{\partial z} \right) + \frac{\partial}{\partial z} \left(2\nu_z \frac{\partial w}{\partial z} \right) \end{aligned}$$

$$\frac{\partial p}{\partial t} + u \frac{\partial p}{\partial x} + w \frac{\partial p}{\partial z} = \frac{\partial}{\partial x} \left(k_x \frac{\partial p}{\partial x} \right) + \frac{\partial}{\partial z} \left(k_z \frac{\partial p}{\partial z} \right)$$

$$\frac{\partial u}{\partial x} + \frac{\partial w}{\partial z} = 0$$

The viscosity consists of a laminar and possibly anisotropic part ν_0 and an eddy viscosity contribution ν_e .

Thus $\nu = \nu_0 + \nu_e$.

The eddy viscosity is prescribed either by a mixing length hypothesis

$$\nu_e = l^2 \Delta \quad \text{where } \Delta^2 = \left(\frac{\partial u_i}{\partial x_j} + \frac{\partial u_j}{\partial x_i} \right)^2$$

$$\frac{1}{l} = \frac{1}{k(z+z_0)} + \frac{1}{\lambda_0}$$

(N.B. u_i are mean fields)

or by a two-equation turbulence model in which

$$\nu_e = q^2 / \epsilon$$

where q is the turbulence kinetic energy and ϵ is the viscous dissipation of turbulent kinetic energy.

The equations for q and ϵ are modelled as

$$\frac{Dq}{Dt} = \left(\frac{q}{\epsilon} \right) \Delta^2 - c_{q1} \epsilon + \frac{\partial}{\partial x} \left(\nu_H \frac{\partial q}{\partial x} \right) + \frac{\partial}{\partial z} \left(\nu_v \frac{\partial q}{\partial z} \right)$$

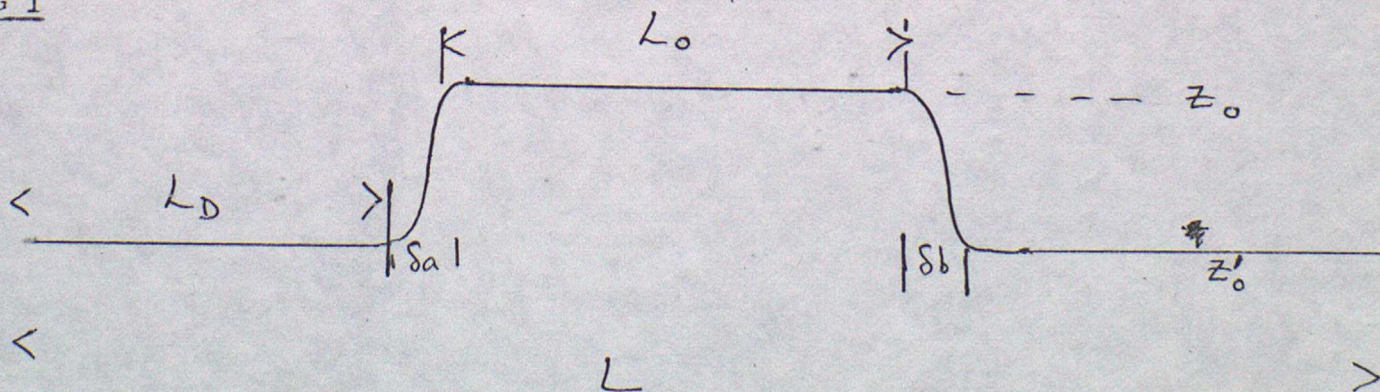
$$\frac{D\epsilon}{Dt} = c_{\epsilon1} q \Delta^2 - c_{\epsilon3} \frac{\epsilon^2}{q} + c_{\epsilon2}^{-1} \left[\frac{\partial}{\partial x} \left(\nu_H \frac{\partial \epsilon}{\partial x} \right) + \frac{\partial}{\partial z} \left(\nu_v \frac{\partial \epsilon}{\partial z} \right) \right]$$

where $\frac{D}{Dt} = \frac{\partial}{\partial t} + u_i \frac{\partial}{\partial x_i}$, differentiation along the mean field.

The viscosity has been expressed in anisotropic form to permit the use of an enhanced horizontal to suppress unwanted physical or numerical instabilities.

A constant pressure gradient $\partial p / \partial y$ is imposed to drive the basic geostrophic flow outside the boundary layer. The distribution of roughness length $z_0(x)$ on the surface $z=0$ is also specified as a function of the six parameters $z_0^B, z_0^T, L_0, L_D, \delta a, \delta b$ and L , the length of the periodic domain. Fig 1 defines these quantities schematically.

FIG 1



The rate of change of z_0 on the curved parts of the graph is that of a \cos^2 function, a smooth profile being chosen to minimise any spurious computational problems due to discontinuities.

The quasi-equilibrium drag on the domain is given by

$$D_E = \int_0^L \tau_0^e(z_0) dx$$

where $\tau_0^e(z_0)$ is the surface stress of a horizontally homogeneous boundary layer in equilibrium with a roughness length of z_0 . The integration is initialised with a 1-D solution appropriate to that value of roughness length \bar{z}_0 such that

$$\tau_0^e(\bar{z}_0) = D_E / L.$$

Thus the amplitude of inertial oscillation is much reduced. Fig 2 shows a comparison of the evolution of the total surface stress

$$D(t) = \int_0^L \tau_0(x, t) dx$$

when this approximate balance is not imposed.

The integration is then continued for a real time ~ 1 hour, where upon only the inertial (long period) oscillation remains. The fields at this stage are treated as steady solutions. The long integrations of Fig 2 suggest that the error in doing this is $\sim 2\%$.

3. Variation of parameters

The parabolic integrations described in the introduction, when scaled with the upstream u'_* and one of the roughness lengths, are functions of the single parameter z'_0/z_0 where $'$ denotes an upstream quantity. The surface stress distribution downstream of a change from rough to smooth in the case $z'_0/z_0 \simeq e^5$ is shown in Fig 3. There is some variation but the models broadly agree in the length scale on which the stress is changing.

Fig 4 shows the corresponding comparisons for the smooth to rough case, $z'_0/z_0 \simeq e^{-5}$. Again there is agreement on the length scale but notice the inflected recovery curve of Shir (1972). Shir used essentially the parameterisation of Petersen (1969) but included the pressure gradients.

An unbounded flow over a step change with a deep model brings in the additional similarity parameter G/fz'_0 , the surface Rossby number and would asymptotically approach equilibrium at the downstream z_0 as $x \rightarrow \infty$.

However we choose to investigate the periodic case. The additional parameters needed to describe the roughness length distribution lead to the following characterisation of the flow

$$\frac{G}{fz'_0}, \frac{L_0}{L}, \frac{z'_0}{L}, \frac{z'_0}{z_0}; \frac{\lambda_0}{D}, \frac{G}{fD}, \frac{\delta a}{L}, \frac{\delta b}{L}$$

where D is the height of the model's stress-free upper boundary, and the following parameters were fixed at

$$\frac{\lambda_0}{D} = \frac{1}{30}, \quad \frac{G}{fD} = 10, \quad \frac{\delta a}{L} = \frac{1}{10} = \frac{\delta b}{L}.$$

The scaling of u_* will be chosen for convenience.

We now show some effects of varying each parameter in turn. The basic parameter values chosen were

$$\frac{G}{fz'_0} = 10^5, \quad \frac{L_0}{L} = .4, \quad \frac{z'_0}{L} = 10^{-3}, \quad \frac{z'_0}{z_0} = 100 \quad (*)$$

Fig 5 shows the friction velocity distribution resulting from a variation of L_0/L . The flow behaves qualitatively as one would expect and does not recover equilibrium even over the smoother surface, consistently with the indications of the parabolic work. However the effect of the varying extent of the rougher surface appears to exhibit more upstream influence. This could not be predicted by the earlier work, although the smooth-rough curve of Shir (1972) may indicate a significant upstream influence associated with an adverse pressure gradient.

Fig 6 shows the effect of allowing $m = z'_0/z_0$ to vary. The difference is principally associated with the difference in equilibrium stress on the smoother surface in each case. The equilibrium is not of course attained, but the equilibrium values are indicated.

Fig 7 shows the effect of varying the surface Rossby number and the difference is again due to the difference in equilibria, which are shown. The shape of the stress recovery curve is very similar in each case. Scaling u_{*k} with one of the equilibrium friction velocities in each case brings the curves into agree-

ment to within 6%. To this level of approximation the dependence on surface Rossby number may be ignorable.

Fig 8 varies z'_0/L while keeping the other parameters constant. This in particular describes the effect of increasing L while keeping L/L_0 and the other dimensional quantities fixed. As one would expect the stress approaches the equilibrium values more closely on the longer L (but does not attain them).

If we consider the results described above, we find that none of the stresses recover equilibrium. However in these cases $L_0/z_0 \lesssim 4 \times 10^5$ which is the order of fetch on which we might expect recovery to occur. To confirm this prediction, suggested by the parabolic models in particular, Fig 11 shows the recovery to equilibrium attained on $L_0/z_0 = 4 \times 10^6$. Thus recovery seems to require fetches of the order $10^6 z_0$.

A direct comparison of the actual u_* distribution with the quasi-equilibrium $u_*^e(z_0(x))$ is shown in Fig 9. The profiles are quite different but the areas under the curves are only 16% different - a quasi-equilibrium estimate of average drag might give a satisfactory first guess. The behaviour of such estimates for a large number of parameter combinations is shown in Table 1. Clearly the estimate is most accurate on the longest length scales, i.e. large

Fig 10a and 10b show comparative results from an integration with the standard $(*)$ parameter set, and alternative parameterisations of the turbulent viscosity γ_e . In the q, ϵ parameterisation described earlier, it is numerically convenient to use a mixing length (ℓ) formulation very low down in the model, where it should be a good approx and give the correct wall behaviour. The difference in surface stress $\sim 4\%$ from the two models, which is within the uncertainty associated with the steady state solution. In Fig 11 the length scale is increased so that $z'_0/L = 10^5$ and then equilibria are achieved but the difference in stress is still $\sim 4\%$, due to $\ell \propto q, \epsilon$ parameterisation.

4. Conclusions

For the range of parameters considered here it seems that in a rough-smooth change the stress recovers in a fetch $\sim 10^6 z_0$ a new equilibrium. For the smooth-rough change our results are compatible with a recovery fetch $\sim 10^4 z_0$. (This is the new z_0 in each case.)

The flows computed here behave simply. They appear to be dominated by advection except in a few cases when near the roughness changes upstream influence and pressure gradients may be significant. Thus the parabolic models should and do give a good approximation to the flow field at medium distances, i.e. not too near the change or too far downstream (when the new equilibrium is being approached). Allied to these considerations it is clear that periodicity does not seem significant in these cases. Attempts to integrate a $z'_0/L = 10^{-2}$ variant of the $(*)$ parameter set, when the flow should feel this effect, were unsuccessful due to computational difficulties.

The different parameterisations used for ν_e were in good agreement but the two-equation turbulence model does have the advantage of not having an "arbitrary" constant like λ_0 in the mixing length formulation, which could conceivably require optimisation for every different flow. The constants in the q, ϵ model can be fixed by considering idealised turbulent flows. However the mixing length parameterisation is less costly to execute and does not have quite such stringent computational constraints.

If average drag is the quantity of interest then a good first approximation is given by the "quasi-equilibrium" value, which improves as $z'_0/L \rightarrow 0$. In practice 10% accuracy can be expected if $z'_0/L \lesssim 10^{-4}$.

References

- E.W. PETERSEN (1969) Modification of mean flow and turbulent energy by a change in surface roughness under condition of neutral stability. QJRMS 95 561-575.
- C.C. SHIR (1972) A numerical computation of air flow over a sudden change of surface roughness. JAS 29 304-310.

References (Contd)

- P.A. TAYLOR (1969) On wind and shear stress profiles above a change in surface roughness. QJPM 95 77-91.
- K.S. RAO et al (1974) The structure of the 2-D internal boundary layer over a sudden change of surface roughness. JAS 31 738-746.

Table 1. Comparison of quasi-equilibrium drag with actual drag.

G/fz'_0	L_0/L	z'_0/L	z'_0/z_0	Actual drag	Q.e. drag	Error %
10^5	.4	10^{-3}	100	$.273 \pm .005$.228	16%
10^5	.2	10^{-3}	100	$.299 \pm .005$.263	12%
10^5	.6	10^{-3}	100	$.245 \pm .005$.193	21%
10^6	.4	10^{-4}	100	$.168 \pm .003$.149	11%
10^5	.4	10^{-3}	10	$.280 \pm .005$.256	9%
10^5	.4	10^{-4}	100	$.258 \pm .005$.228	12%
$10^5 (*)$.4	10^{-5}	100	$.237 \pm .002$.228	4%
$10^5 (*)$.4	10^{-4}	100	$.248 \pm .003$.228	8%

(*) Low resolution; $\frac{1}{2}$ resolution of others.

In all runs the remaining dimensionless parameters were

$$\lambda_0/D = 1/30 \quad ; \quad G/fD = 10 ;$$

$$\delta a/L = 1/10 \quad ; \quad \delta b/L = 1/10 .$$

Comprehensive Legends

Fig. 2 $\frac{G}{f z_0'} = 10^5$ $\frac{L_0}{L} = .4$ $\frac{z_0'}{L} = 10^{-4}$ $\frac{z_0'}{z_0} = 100$

comparisons of initialisation, balanced drag or not.

Fig. 3. Parabolic similarity. Rough-smooth.

Fig. 4. " " Smooth-rough.

Figs. 5-9. $\frac{G}{f z_0'} = 10^5$. $\frac{L_0}{L} = .4$. $\frac{z_0'}{L} = 10^{-3}$. $\frac{z_0'}{z_0} = 100$ (*)

Fig. 5. (*) but with $\frac{L_0}{L} = .2, .4, .6$.

Fig. 6. (*) but with $z_0'/z_0 = 10, 100$.

Fig. 7. (*) $G/f z_0' = 10^5, 10^6$.

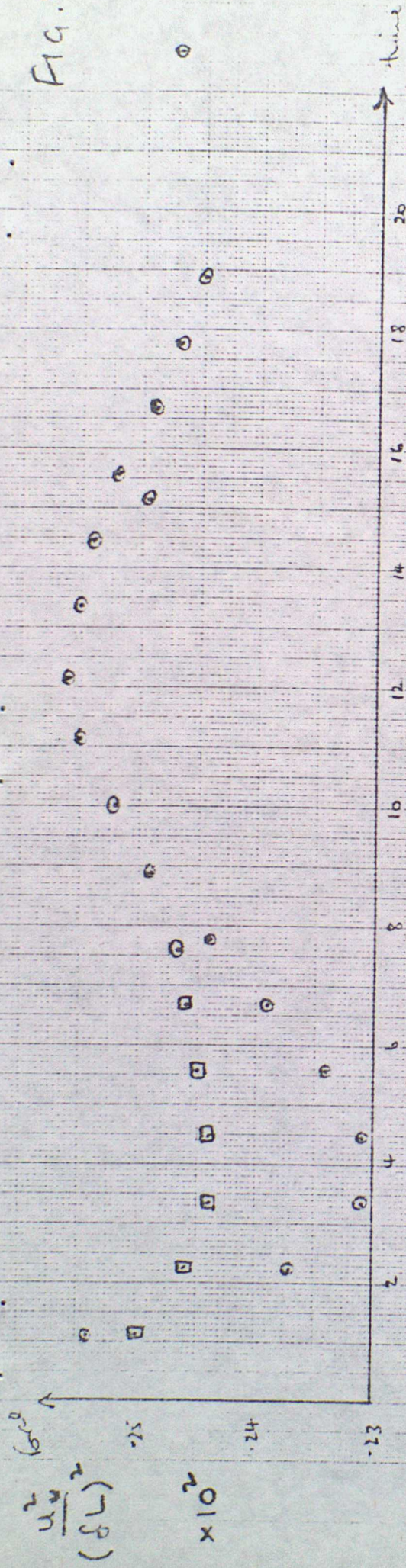
Fig. 8. (*) $z_0'/L = 10^{-3}, 10^{-4}$.

Fig. 9. (*) compared with quasi-equilibrium.

Fig. 10(a) Variation of u_w with x , for L and q, t , on (*).

10(b) Time evolution of average force for same comparison.

Fig. 2.



Oscillation with time
of Average surface stress.

$\Delta t = 4s$

$\Delta t = 8s$

$\Delta t = 4s$



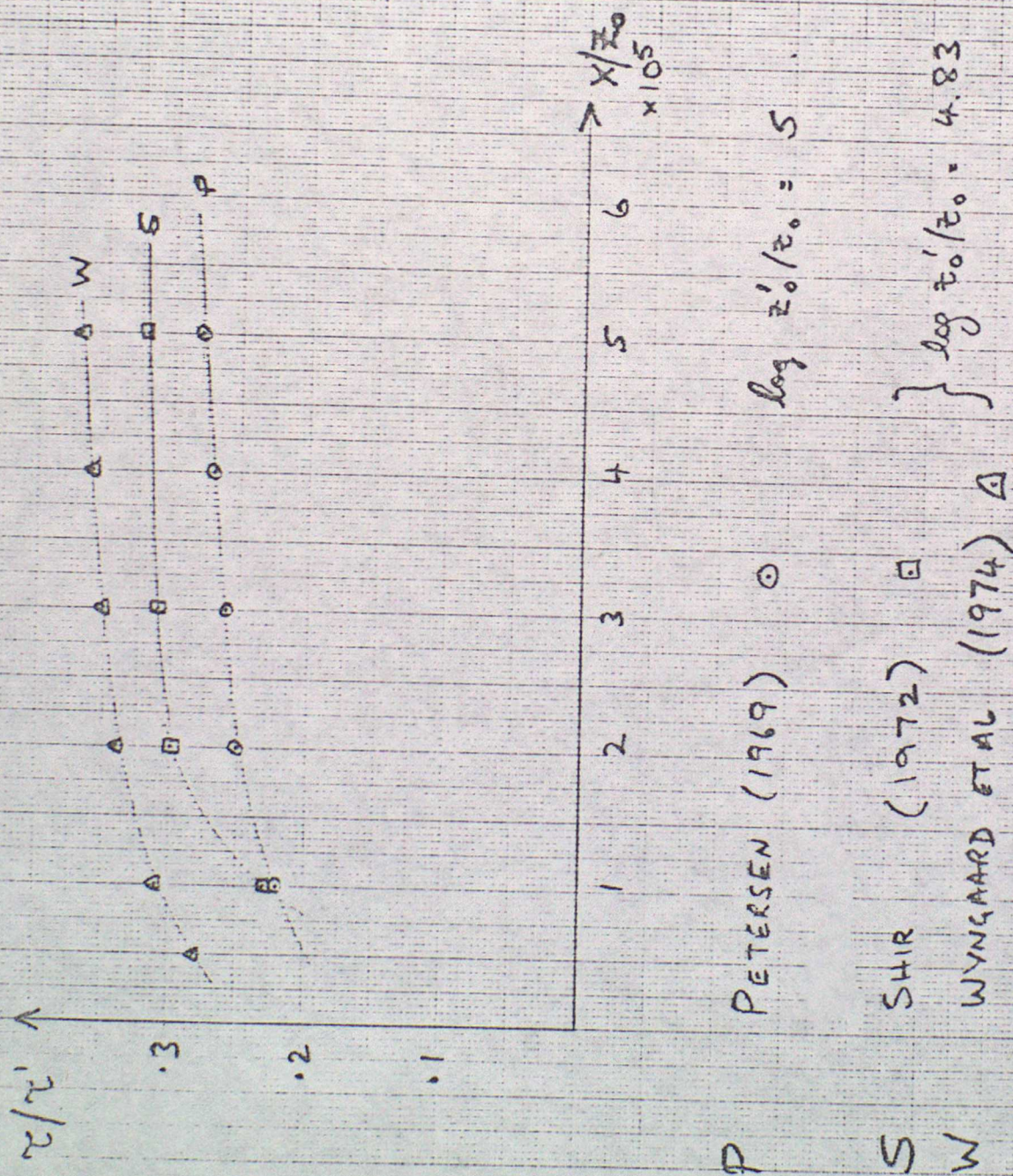
$\tau_0 = 0.01$

$\tau_0 = .18$

Note: balance

Approx. balance

Fig. 2.



DEVELOPMENT OF

SURFACE STRESS

WITH FETCH DOWNSTREAM

OF A CHANGE IN SURFACE

ROUGHNESS.

(PARABOLIC MODELS)

ROUGH - SMOOTH.

Fig. 4.

As Fig. 3

SMOOTH -
ROUGH

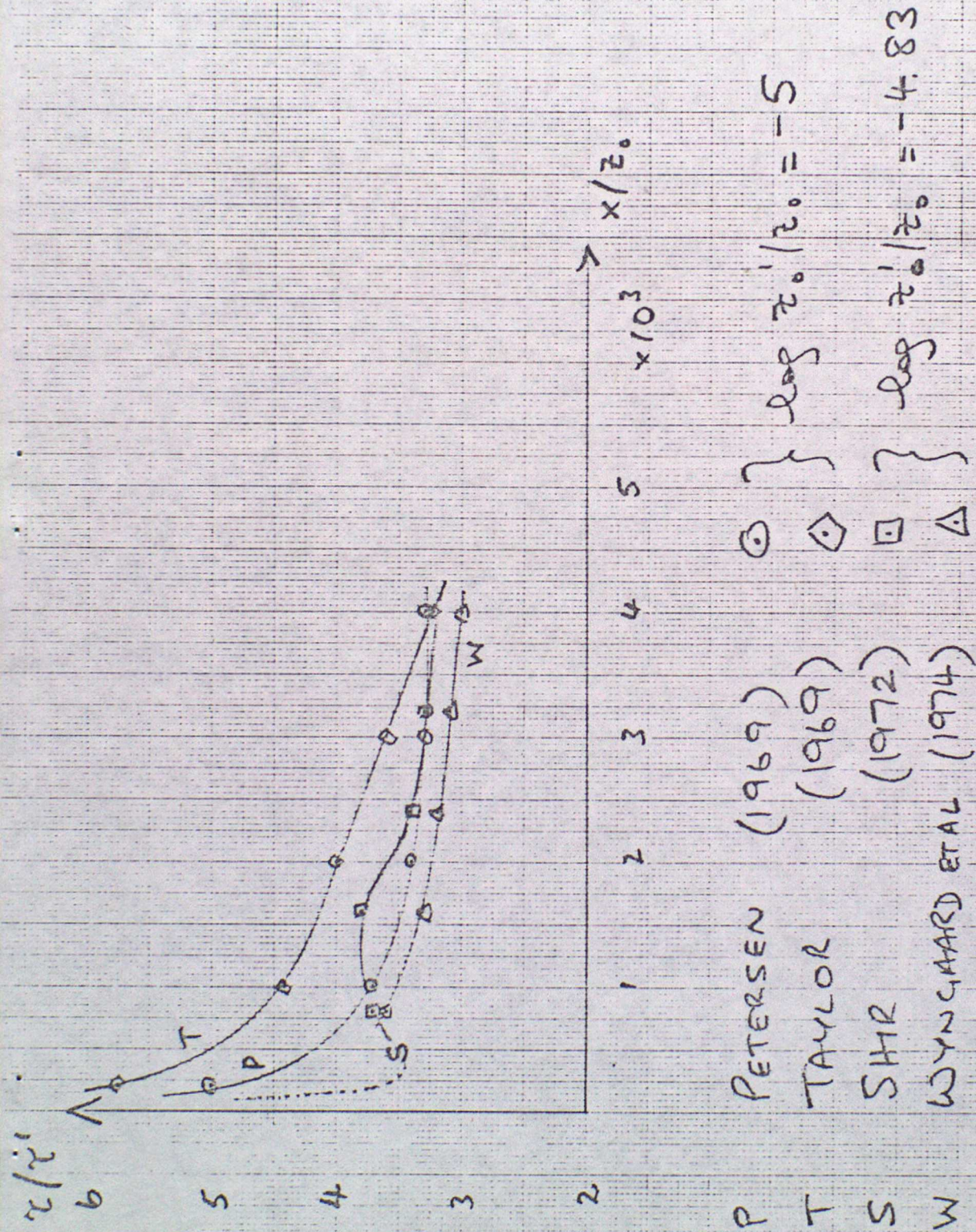



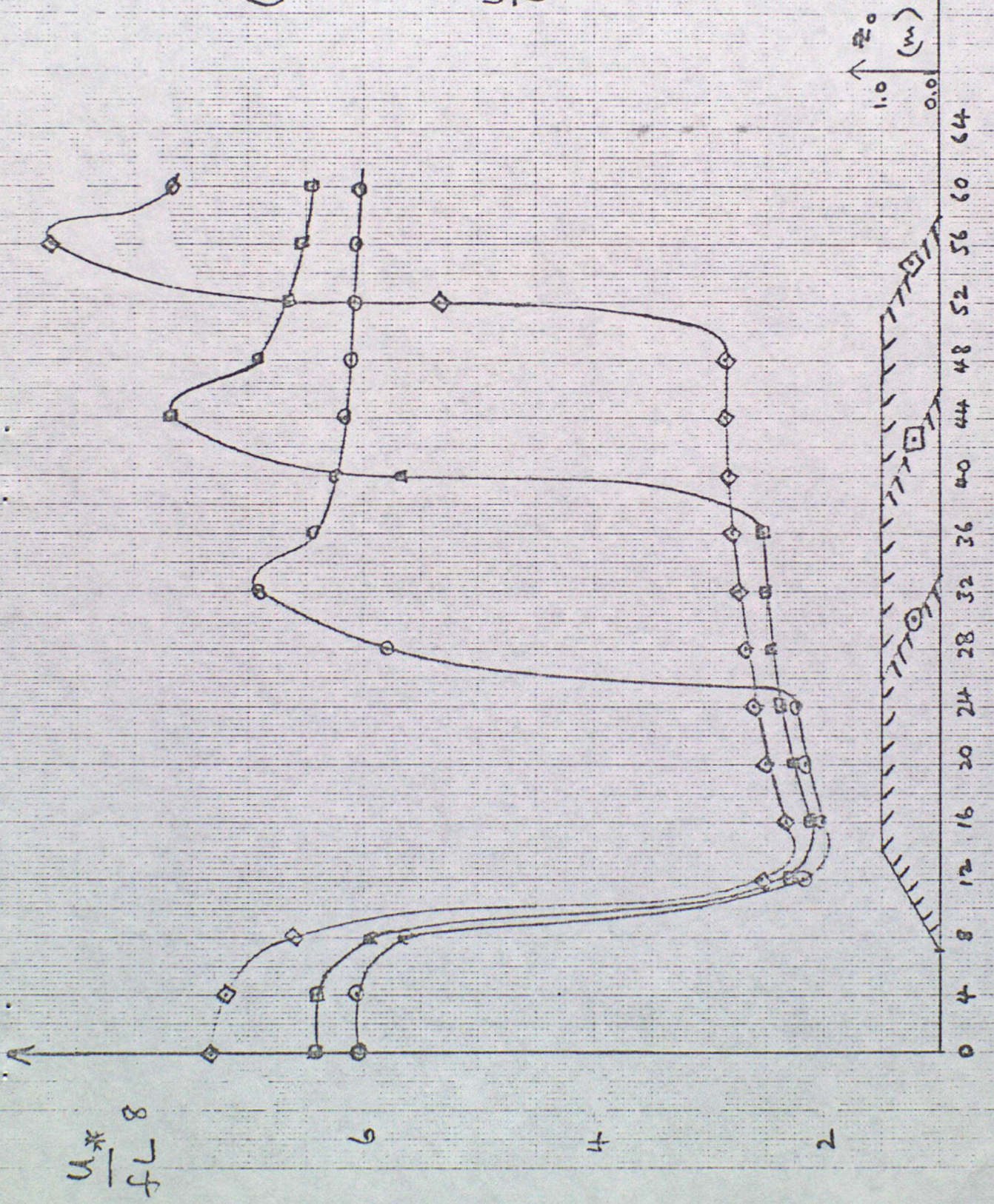


Fig. 5

(Approx.) Steady State
 u_x distribution

Effect of varying $\frac{L_0}{L}$

$\frac{L_0}{L} = 0$	$\frac{L_0}{L} = 0.2$	$\frac{L_0}{L} = 0.4$	$\frac{L_0}{L} = 0.6$
			



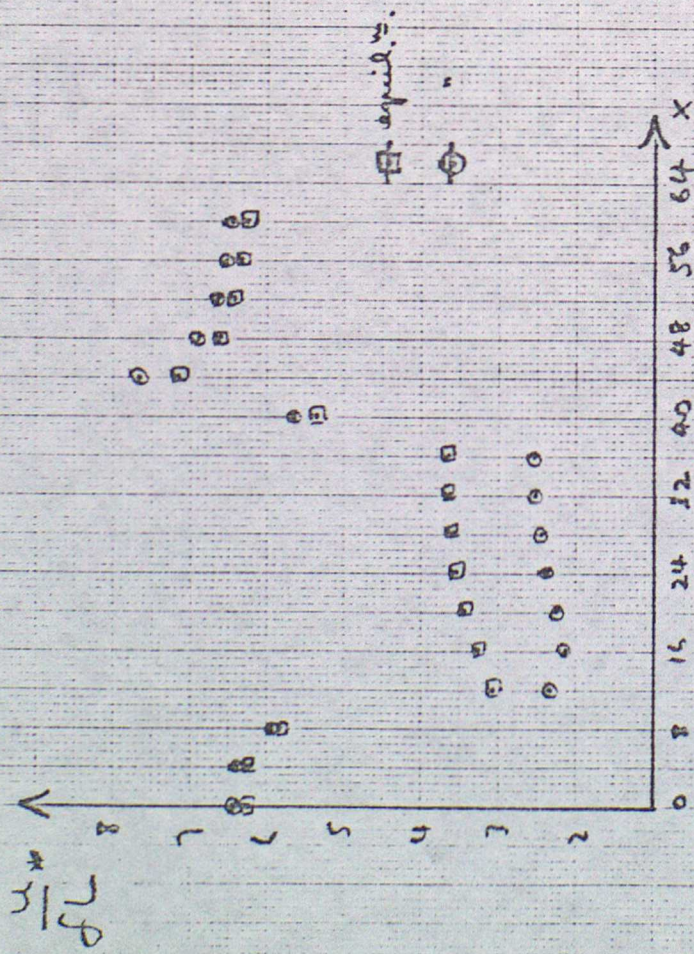


Fig. 6. Varying m .

Steady state u^* distn.

- $m = 100$
- $m = 10$

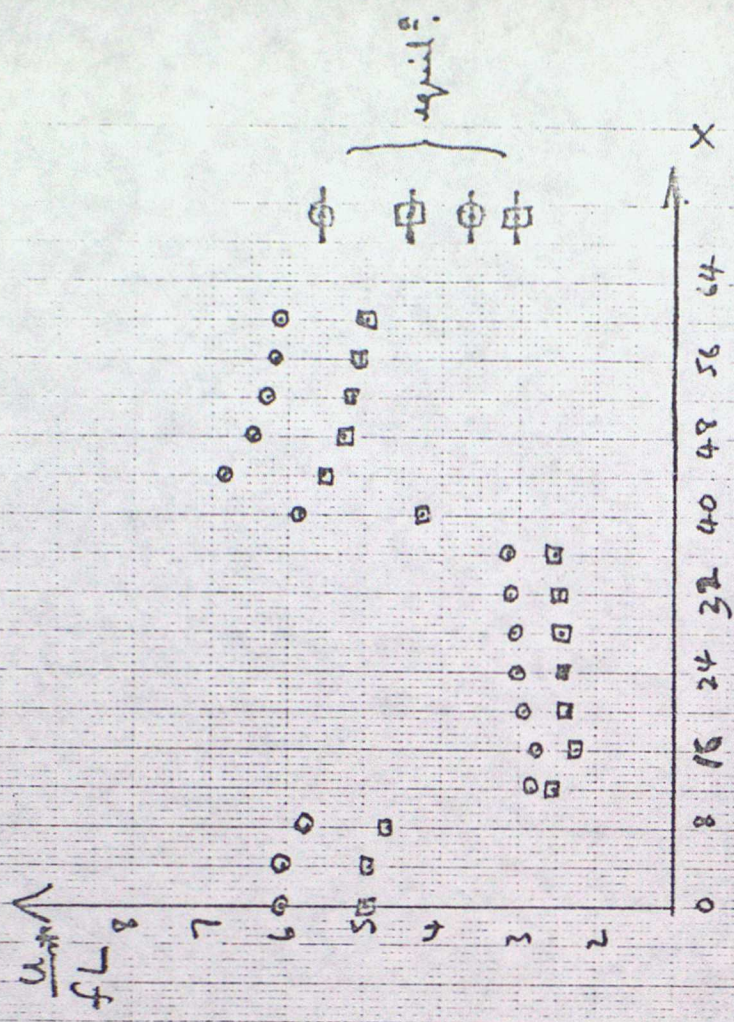


Fig. 7. Varying G/fz'_0 .

Steady state u^* distn.

- $G/fz'_0 = 10^5$
- $G/fz'_0 = 10^6$

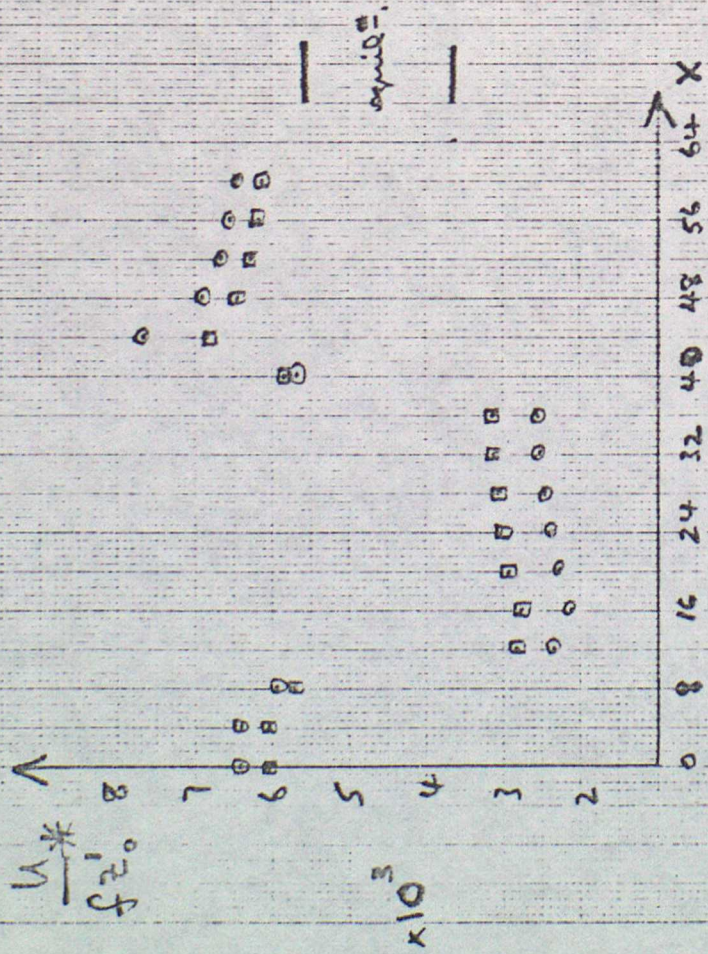


Fig. 8. Varying $\frac{z_0'}{L}$.

○ $\frac{z_0'}{L} = 10^{-3}$

□ $\frac{z_0'}{L} = 10^{-4}$

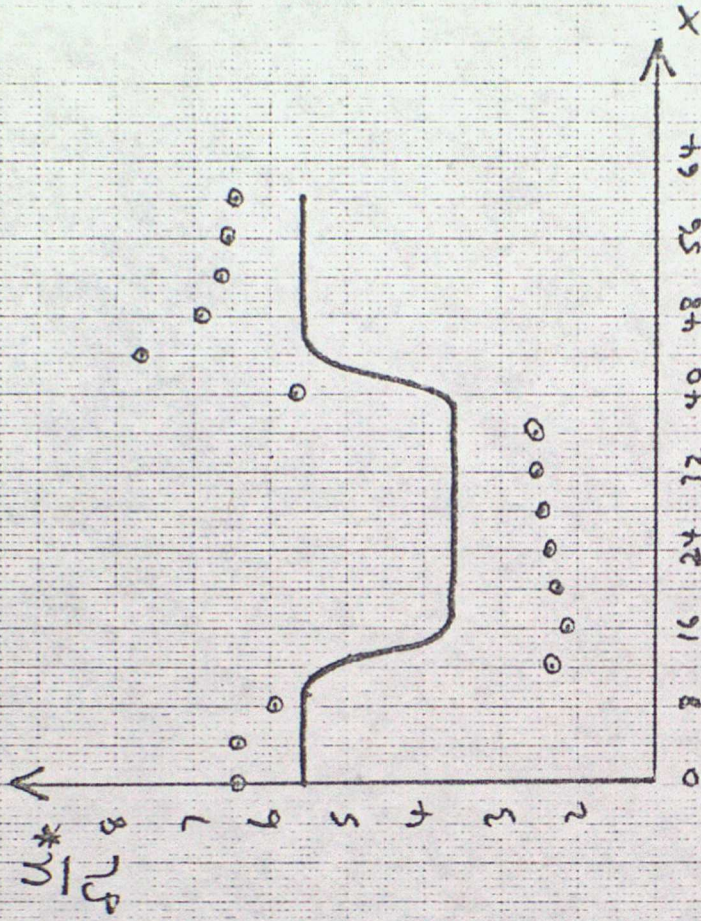


Fig. 9. Comparison of equilibrium with the actual steady solution.

— Quasi-equilibrium.

○ Steady state

Parameters as other Figs.

Fig. 10 am

$$\frac{\Delta u}{\Delta L}$$

Variation in x of surface
friction velocity u_{*0}

cf. L and q_{*E}

L
 q_{*E}

Δu_{*0} comparable / consistent with
4% difference in stress.

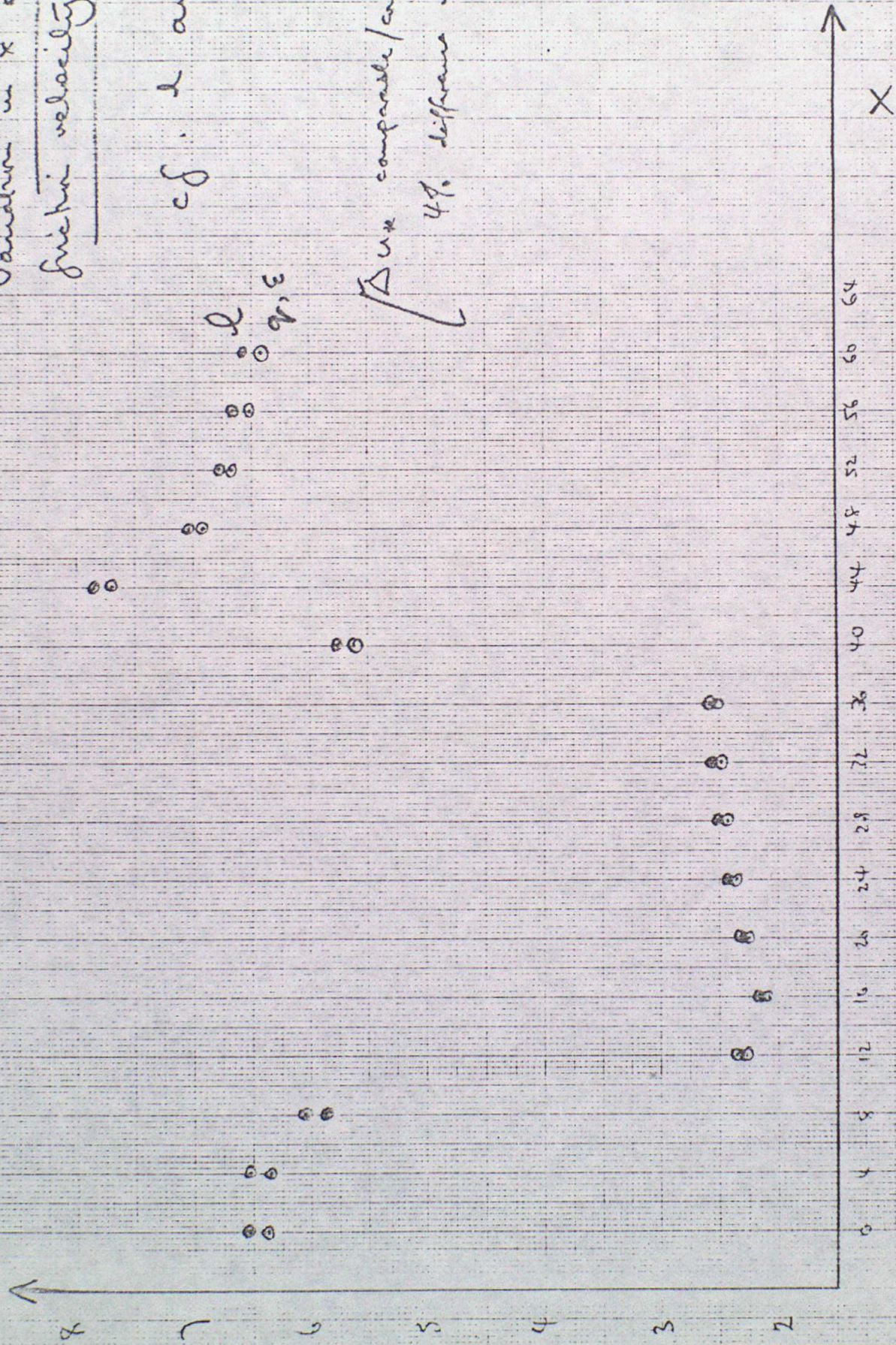


Fig. 106

Variation of average force with time

cf. ℓ and q, ϵ .

N.B. q, ϵ essentially constant

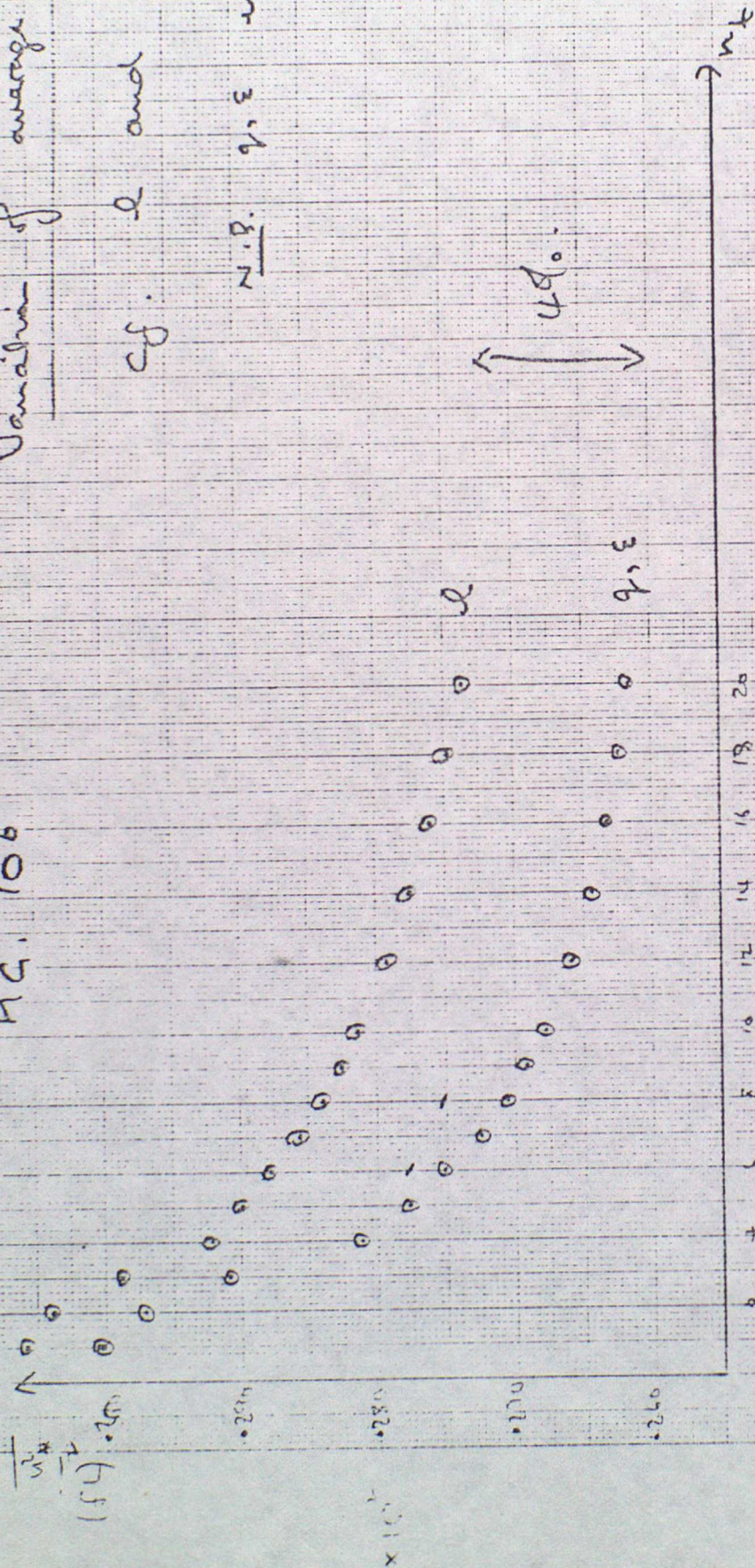


Fig. 11

Surface stress $\sigma = 10^5 \text{ m.}$
 Write ϵ and q, ϵ .

$\epsilon = 10^{-5}$

